Dangling bond deflection model: Growth of gel network with loop structure

Hang-Shing Ma,[1,*] Rémi Jullien,[2] and George W. Scherer[3]
[1]*Department of Chemical Engineering, Princeton University, Princeton, New Jersey 08544*
[2]*Laboratoire des Verres, UMR 5587, CNRS, Université Montpellier II, Place Eugene Bataillon, 34095 Montpellier cédex 5, France*
[3]*Department of Civil and Environmental Engineering, Princeton University, Princeton, New Jersey 08544*
(Received 10 July 2001; published 3 April 2002)

It has been shown that the closed-loop structure in the model gel networks is responsible for their stiffness. However, the creation of loops has been underestimated in most of the existing kinetic aggregation models [e.g., DLCA (diffusion-limited cluster-cluster aggregation) and derivatives]. A dangling bond deflection (DEF) mechanism is proposed to model the fluctuation of dangling branches or dead ends under thermal excitation. The random deflections of the dangling branches can create loops in the network by forming intracluster bonds, and proceed during both the gelling and aging processes. The resulting DLCADEF networks have extensive loop structure with a negligible number of dangling branches. Its growth kinetics and fractal behavior resemble those of real gels, including volume-invariant gel time and fractal dimension of about 2. The DLCADEF model is the first attempt to model the gel growth with loop formation by the physically realistic fluctuation mechanism. The mechanical properties of the resulting networks will be studied and verified by comparison with real gels.

DOI: 10.1103/PhysRevE.65.041403 PACS number(s): 61.43.Hv

I. INTRODUCTION

The aggregation of polymeric or colloidal particles to form sparse clusters or gel networks is a common natural phenomenon, and is important in materials processing [1]. The properties and applicabilities of such aggregation-derived materials depend on their structural characteristics. However, the structure of these aggregates is highly disordered [2]; therefore, it is difficult to describe the structure quantitatively. In addition, the sparse networks are usually too compliant to sustain themselves without excessive deformation during experimental characterization [3], hence intensifying the challenge to reveal their structure. As a result, the ''true'' structure and its implications for the mechanical properties of these sol-gel derived materials, e.g., aerogels, is not yet theoretically understood. The mystery can be alleviated by numerical computation to model the random aggregation process, from which the aggregate structure can be simulated and its properties can be derived mathematically. A physically realistic aggregation model, therefore, becomes essential to grow the structure that can represent the real cluster or gel network. The introduction of the ''dangling bond deflection'' model is to simulate an important movement of flexible branches in the network. By implementing it together with the conventional aggregation model, a more realistic gel network with extensive loop structure can be generated.

Percolation theory has been invoked to account for the gelation process [4], but was contradicted by the unrealistically high scaling exponent of modulus against density predicted by the theory [5]. Diffusion-limited cluster-cluster aggregation (DLCA) [6,7] was regarded as the first model to simulate the sol-gel transition. There are many derivatives developed to account for aggregation under different reaction conditions, e.g., reaction-limited cluster-cluster aggregation [8] and finite interparticle binding energetics [9]. More aggregation models are reviewed in Ref. [10]. The agreement of the various models with reality was usually validated by comparison with the experimental results on the growth kinetics (e.g., the evolution of cluster size distribution, extent of reaction) and the fractal geometry of the aggregate products [1,11].

Despite the rich variety of the aggregation models, few works have been done to elucidate the structure-property relationship of such randomly aggregated materials. The present authors have attempted to use the finite element method to measure the linear bulk modulus of on-lattice DLCA networks [12]. The abundance of dead ends on the DLCA networks leads to an unrealistically high scaling exponent $m=7.6$ in the well-known scaling relationship of aerogels

$$K \propto \rho^m, \tag{1}$$

where K is the bulk modulus, ρ is the relative density, and m is the scaling exponent usually between 3 and 4 in the experiment [12,13]. After trimming the dead ends, the networks are left with a structure consisting mainly of loops with much lower density, ρ_L. These networks obey

$$K \propto \rho_L^{3.6}, \tag{2}$$

which agrees with the experimental results. Therefore, we conclude that the loop structure in the trimmed DLCA and real gel networks accounts for their stiffness. Most of the past aggregation models were developed with insufficient emphasis on loop formation during gelation. As a result, they fail to explain the stiffness of the real gel network. To create a structure possessing the mechanical properties of the real gel network, a physically realistic mechanism of cluster movement capable of creating loops in the network must be

*Corresponding author.
Email address: hangma@Princeton.edu

included in the aggregation model. The first effort to include deformation, and consequently loop creation, during aggregation was initiated by one of the authors in the fluctuating bond aggregation model [14,15]. However, the model was built upon the on-lattice DLCA model, and so it is less applicable for studying mechanical structure-property relationship.

The concept of bond fluctuation is extended to the development of the dangling bond deflection (DEF) model that imposes tiny deflections on the dangling bonds of the diffusing clusters during aggregation. A dangling bond serves as the only bond connecting a (dangling) branch of particles to a cluster, and the dangling branches are created by the random aggregation of particles in the off-lattice DLCA process. The deflection motion simulates the thermally activated fluctuation of the dangling branch about its equilibrium position with reference to its dangling bond. When the deflecting branch collides with the rest of the same cluster, a loop within the cluster is formed by irreversible bonding between the colliding particles. By combining the off-lattice DLCA model with the DEF, a gel network with loop structure can be generated from a random dispersion of particles. If the simulation is allowed to continue after the aggregation is completed, most of the dangling branches are transformed into loops, and the resulting structure is the subject of this study. The DLCADEF model is developed as the first step towards realistic modeling of the growth of a gel network that can account for the mechanical properties of gels. More detailed explanation of the model and the justification of the assumptions are presented in Sec. II. The growth kinetics, fractal geometry, and vibrational spectrum of the resulting structure are discussed in Sec. III.

II. DLCADEF MODEL

A. DLCA (diffusion-limited cluster-cluster aggregation)

The DLCA model implemented here is based on the three-dimensional off-lattice extension [16] of the original DLCA model [6,7]. The modeling begins by dispersing n_p spherical particles of unit diameter into a cube of edge length b using the sequential addition method, so that these spheres are neither touching nor overlapping with one another. The number n_p is estimated by

$$n_p = \frac{6}{\pi}\rho b^3, \tag{3}$$

with the designated relative density ρ for the resulting network. The (ρ,b) of the model gel networks studied are (0.018,159), (0.03,100), (0.056,79), (0.1,63), and (0.18,50). The box size decreases with increasing density to maintain a ratio of approximately 10:1 between b and the mass correlation length ξ of the network. The estimation and the density dependence of ξ will be presented in Sec. III.

A particle or cluster of particles is randomly selected at each iteration to undergo a translational displacement in a randomly chosen direction. The probability $P_t(i)$ of picking the cluster i out of total number of clusters n_c depends on the number distribution of the clusters assuming the clusters possess a fractal dimension of 2 [6,7], i.e.,

$$P_t(i) = \frac{n_{\mathrm{pc}}(i)^{-1/2}}{\sum_{j=1}^{n_c} n_{\mathrm{pc}}(j)^{-1/2}}, \tag{4}$$

where $n_{\mathrm{pc}}(j)$ is the number of particles in cluster j. A slight variation in the fractal dimension and thus the exponent of $n_{\mathrm{pc}}(j)$ does not affect the results. The displacement is a unit particle diameter unless the moving particle or cluster collides with another particle. If so the moving cluster stops right at the collision, and a new bond is formed between the two touching particles. Periodic boundary conditions are implemented so that particles moving out of the box reenter through the opposite side. This translational Brownian motion ends when all the particles are aggregated into one single cluster.

B. DEF (dangling bond deflection)

Analogous to the branches of a tree waving in the wind, the particles in the clusters fluctuate about their equilibrium positions by thermal energy. The DEF model simulates this motion in the aggregates by performing small deflections of dangling bonds. A dangling bond is defined as an interparticle bond connecting a dangling branch of a particle or cluster with another cluster. If the dangling bond is cleaved, the dangling branch becomes isolated. The deflection is performed by randomly choosing a dangling bond $\overrightarrow{OA}$ and a unit vector $\overrightarrow{OW}$ as the axis of rotation. The position O represents the particle at one end of the dangling bond that serves as the origin of rotation, and A is the particle at the other end, meaning that $\overrightarrow{OA}$ and $\overrightarrow{AO}$ refer to two separate dangling bonds. The dangling branch associated with dangling bond $\overrightarrow{OA}$ is the cluster connected to particle A (including A) other than the particle O. This branch is then rotated about $\overrightarrow{OW}$ by a constant angle θ. For a particle within the dangling branch with an initial positional vector $\overrightarrow{OK}_i$, its final position $\overrightarrow{OK}_f$ is given by

$$\overrightarrow{OH} = (\overrightarrow{OK}_i \cdot \overrightarrow{OW})\overrightarrow{OW}, \tag{5a}$$

$$\overrightarrow{HK}_i = \overrightarrow{OK}_i - \overrightarrow{OH}, \tag{5b}$$

$$\overrightarrow{HU} = \overrightarrow{OW} \times \overrightarrow{HK}_i, \tag{5c}$$

$$\overrightarrow{OK}_f = \overrightarrow{OH} + \overrightarrow{HK}_i \cos\theta + \overrightarrow{HU} \sin\theta, \tag{5d}$$

where $\overrightarrow{OH}$ is defined as the projection of $\overrightarrow{OK}_i$ onto $\overrightarrow{OW}$. The angle θ is chosen as $\pi/100$ rad that is small enough to keep the maximum particle displacement (i.e., $|\overrightarrow{K_iK_f}|$) comparable to or lower than a unit particle diameter even during the rotation of a large dangling branch. The probability $P_r(i)$ of picking a dangling branch i out of total number of dangling

branches n_{db} again depends on the mass distribution of the dangling branches (derivations are shown in the Appendix A), and is defined as

$$P_r(i) = \frac{n_{\mathrm{pd}}(i)^{3/2}}{\sum_{j=1}^{n_{\mathrm{db}}} n_{\mathrm{pd}}(j)^{3/2}}, \tag{6}$$

where $n_{\mathrm{pd}}(j)$ is the number of particles in the dangling branch j. The heavier branches are less likely to deflect.

When the dangling branch runs into another particle during rotation, the rotation will stop at the point when two particles first touch each other, before reaching the angle θ. If the two bonding particles belong to the same cluster, a loop within the cluster is closed, and every bond constituting the loop is declared nondangling. In other words, if a bond within the loop is cleaved, the cluster will still be connected as one piece. In this model, we assume that the bonds constituting the loops do not participate in the deflection motion. This is a quite reasonable assumption as such bonds are more efficiently connected against fluctuations, therefore, they are more hindered than the dangling bonds. In reality, deflections within the loops are possible, but to the first approximation these movements are ignored. If the cluster is larger than the size of the box, the deflection motion of a dangling branch in such a cluster may stick one end of it to the other end through the periodic boundary conditions. Then a ''periodic'' backbone extending from one side of the box to the other side is formed and the bonds making up the backbone are classified as nondangling. Moreover, the formation of the backbone can be used as a measure of the gel point, which is defined as the time when the clusters start to percolate and span the volume of the system. The coordination number of each particle is limited to four, and any movement that leads to bond formation of an already saturated particle is rejected. Creation of loops in the gel network by thermally activated swaying of dangling branches is realistic and significant in the growth process, and this mechanism is approximated by the dangling bond deflections for the modeling of sol-gel transition.

C. DLCADEF (combination of DLCA and DEF)

The two models (DLCA and DEF) represent two different cluster movement mechanisms. By combining them, a diffusion-limited cluster-cluster aggregate structure with loops can be simulated. The process is summarized in a two-dimensional illustration shown in Fig. 1. At each iteration, the choice of either DLCA or DEF mechanism depends on their relative frequencies of occurrence. The parameters ω_t and ω_r can be interpreted as the summation of the relative frequencies of occurrence of the cluster's translational displacement and the dangling branch's rotational movement, respectively. They are defined as

$$\omega_t = \sum_{i=1}^{n_c} n_{\mathrm{pc}}(i)^{-1/2}, \tag{7a}$$

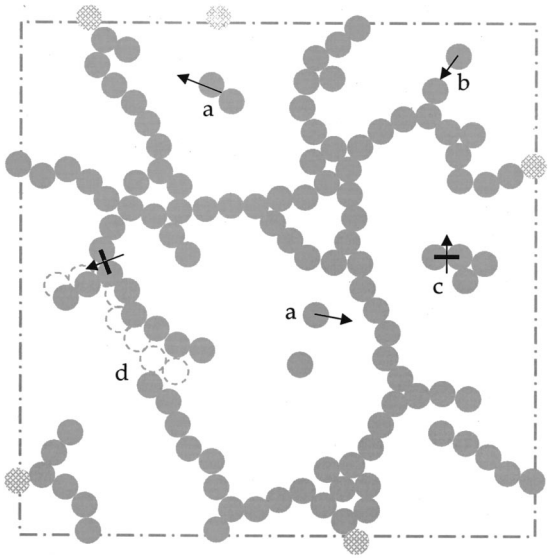

FIG. 1. Two-dimensional (2D) illustration of 3D DLCADEF modeling. (a) Translational random trajectories of particles and clusters. (b) Dangling bond formation by sticking of particles or clusters. (c) Dangling bond deflection: (i) both sides of the bond can be dangling branches; (ii) only one branch is chosen to deflect at a time. (d) Loop formation by forming an intracluster bond.

$$\omega_r = \sum_{i=1}^{n_{\mathrm{db}}} n_{\mathrm{pd}}(i)^{-3/2}, \tag{7b}$$

and are equivalent to the denominators of Eqs. (4) and (6), respectively. The probability P of having the DLCA mechanism operate at each iteration is such that

$$P = \frac{\omega_t}{\omega_t + F\omega_r}, \tag{8}$$

while for DEF the probability is $(1-P)$. The parameter F is the weighting factor of the two relative frequencies, and the physical motivation of the choices of magnitude of F is given in the Appendix B. A time scale t is defined such that at each iteration, the clock is incremented by a small time δt, which is defined as

$$\delta t = \frac{1}{\omega_t + F\omega_r}. \tag{9}$$

To investigate the effect of F on the growth mechanism, largely different values of $F=10$, 100, and 1000 are used to create the DLCADEF networks, together with $F=0$ that reduces the model to a purely DLCA process. As a result, F can also be interpreted as the compliance of the bonds, such that when $F=0$ the bonds are too stiff to deflect, and the readiness of deflection increases with F. When F is set above zero, the modeling is allowed to proceed after the aggregation has completed until less than 0.1% of the particles on the network belong to dangling branches.

The simulations were carried out on a silicon graphics IRIX server with 270 MHz IP27 processors, and a LINUX workstation with 550 MHz Intel P3 processors. The program

runs on a single processor, and requires as much as 4 GB of memory and two weeks of computation time for a realization of a DLCADEF network.

III. NETWORK STRUCTURE

A. Appearance

The most direct way to analyze the network structures is to ''look'' at them. Slab views of the model at $\rho=0.03$, 0.056 and $F=0$, 10, 100, and 1000 with a depth of view of 10 units of particle diameter are shown in Fig. 2. The particles in the aggregates of $F=0$ are more scattered than those in the other F's. The difference can be rationalized by the presence of the dangling bond deflections in the $F>0$ networks. By the end of the simulation, the dangling branches abundant in the $F=0$ models are mostly collapsed onto the backbone of the networks to form loops. As a result, bigger pores and denser blobs of particles are observed in the DLCADEF networks of $F>0$. There is not any apparent difference between the networks of different nonzero F's. The network growth has the same termination condition, which converts most of the dead ends into loops. Therefore, any $F>0$ network, regardless of the magnitude, becomes an interconnection of dense blobs that comprise cyclic chains of particles.

B. Growth kinetics

The evolutions of the average number of particles in a cluster $\langle n_{pc}\rangle$ and the number of dangling bonds n_{db} with Monte Carlo time t are illustrated in Fig. 3 for $\rho=0.056$ and $b=79$. It was shown that the DLCA model agrees with Smoluchowski's equation of aggregation kinetics at the early stage of growth [1,11]. The $\langle n_{pc}\rangle$ can be derived from Smoluchowski's equation in the form

$$\langle n_{pc}\rangle = 1 + 0.5\frac{t}{\tau}, \tag{10}$$

where τ is the characteristic time of dimer formation, and equals 1 in the DLCA model [11]. The correct τ is recovered in the DLCA model in this study as shown in Fig. 3(a), justifying the definition of the Monte Carlo time. However, the τ decreases with increasing F in the model because more restructuring than aggregation takes place at a higher F by the dangling bond deflections within the clusters.

The number of dangling bonds increases monotonically with time for $F=0$, as shown in Fig. 3(b). However, for the $F>0$ networks, the n_{db} rises to a maximum point shortly after the beginning of aggregation, and then declines to almost zero at the end of the simulation. There is a dip in the n_{db} occurring at time t, which is larger for networks with a smaller F, except for $F=0$. This happens when the formation of a periodic backbone converts a large number of the originally dangling bonds to nondangling bonds, given that they belong to the backbone. As a result, the time at which the dip takes place is regarded as the gel point t_{gel}.

The t_{gel} occurs at a low $\langle n_{pc}\rangle$ because of the highly heterogeneous distribution of cluster size during the aggregation, such that the spanning cluster is present when there are still numerous oligomers around, thus suppressing the value of $\langle n_{pc}\rangle$. The variation of gel point versus density and F is illustrated in Fig. 4. The t_{gel}'s were verified with realizations at half of the designated box size at each density, which all showed negligible size-dependent effects. The t_{gel} decreases with increasing density in almost a power-law fashion. The shortening of t_{gel} with increasing F becomes apparent when $\rho \geqslant 0.056$. This can be rationalized by the fact that dangling bond deflections can lead to polymerization in addition to loop formation, when the deflecting branch collides with a neighboring cluster. This phenomenon is apparent when the clusters are crowded together, especially at high density. Therefore, when both ρ and F are high, the largest cluster in the simulation, which normally has also the largest amount of dangling bonds, can grow in size much faster than one with a lower F. As a result, this cluster starts to span the volume much earlier and at a much lower $\langle n_{pc}\rangle$, as illustrated in Fig. 3(a).

C. Degree of cross linking

The degree of cross linking can be illustrated by the probability distribution of the coordination number of particles in the network, as shown in Fig. 5. Particles within a linear chain have coordination number of 2, while those acting as the branch units have coordination number of 3 or 4. Particles with coordination number of 1 represent monomeric dead ends. For $F>0$, the networks have negligible dead ends, and more branching as density decreases. The degree of branching increases also with increasing F as more dangling bond deflection takes place at the early stage of aggregation. Since the dangling branches of the young primary clusters are small, the loops formed are small and the coordination number becomes high. However, as density increases, the primary clusters are more crowded together. They are likely to percolate and lock up the dangling branches before the branches can deflect freely to form dense and small loops. Therefore, the coordination number decreases.

D. Pair correlation

The gel networks obtained from the DLCA model exhibit a fractal structure [11,16], as do the real fractal aggregates in aerogels [17]. The fractal dimension d_f and the correlation length ξ can be estimated from the model gel network by measuring its pair-correlation function $g(r)$ defined as

$$g(r) = \frac{\pi/6}{\rho}\frac{1}{4\pi r^2}\frac{\delta n}{\delta r} = \frac{1}{24\rho r^2}\frac{\delta n}{\delta r}, \tag{11}$$

where δn is the number of spherical particles, located within the spherical shell at a distance between r and $r+\delta r$ from a particle. The ρ term in Eq. (11) normalizes $g(r)$ to 1 when the length scale r becomes so large that the network appears to be homogeneous in density. The $g(r)$'s of $F=0$ and 100 at $\rho=0.03$ are illustrated in Fig. 6, which are averaged from all the particles in the five realizations of each (ρ,b,F) combination. A comprehensive analysis of the pair correlation of the DLCA networks was given in Refs. [16] and [18]. There

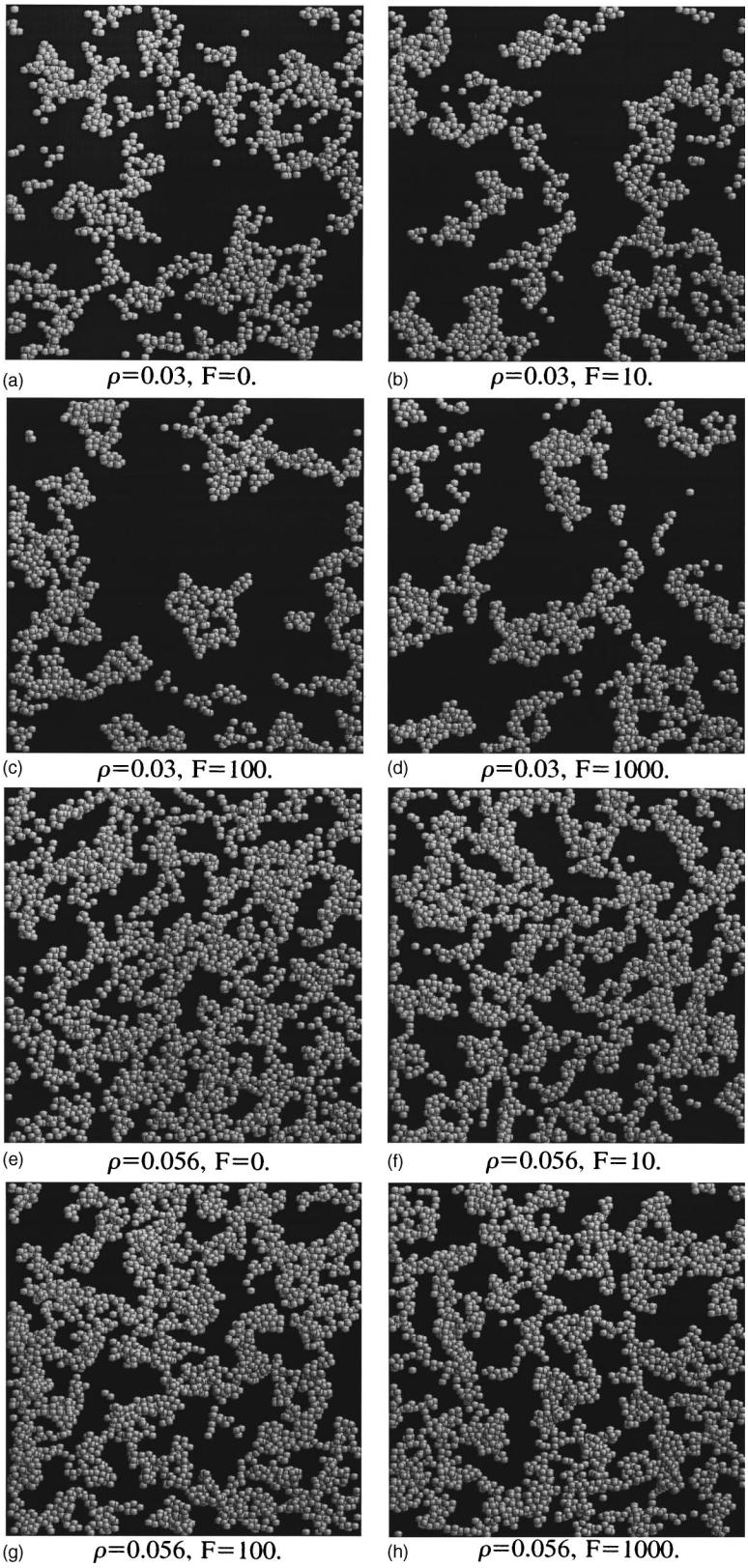

FIG. 2. 50 (length)×50 (width)×10 (depth) slab view of some DLCADEF model gel networks in the form of particle aggregates.

is a minimum in each $g(r)$ separating the fractal and homogeneous regimes, and the minimum is defined as the mass correlation length ξ. The fractal dimension d_f can be evaluated from the volume integral of $g(r)$, defined as $f(r)$,

$$f(r)=\int_0^r g(r)4\pi r^2\,dr\propto r^{d_f}, \tag{12}$$

which scales with the distance $r<\xi$ with the exponent d_f. An illustration of how d_f is evaluated from $f(r)$ is shown in Fig. 7 for $F=0$, 100 and $\rho=0.03$. Although ξ is about 10, only the regime between 3 and 6 is considered as fractal to avoid the crossover effect towards ξ and singularities below 3.

The variation of d_f with ρ is illustrated in Fig. 8, with the fractal range at each ρ from which d_f are evaluated. The d_f's of the DLCA networks agree with the results in Ref. [18]. The monotonic increase of d_f with ρ in the DLCA network is captured also in the $F>0$ DLCADEF networks. The higher d_f than the classical value of 1.8 in the single-cluster DLCA model [10,11] is due to the crossover effect—the interpenetration of the clusters in the finite-density systems. However, the values of the $F>0$ DLCADEF networks are apparently lower than those of the DLCA networks at the same density, although they are fairly insensitive to the magnitude of F. The lower d_f can be accounted for by the compaction effect of the DEF mechanism on the network. Dense blobs of particles are created by formation of small cyclic structures due to dangling bond deflections. The higher local density within the blobs lead to steeper drop of density away from them, which is equivalent to a smaller fractal dimension.

The variation of ξ with ρ and F is illustrated in Fig. 9, which shows that the mass correlation length increases with decreasing density. Comparatively, the dependence of ξ on F is much less sensitive. The minima in $g(r)$'s of the $F>0$ DLCADEF networks are always deeper than those of the DLCA networks. The depth can be attributed to the compaction effect of the dangling bond deflections that form dense blobs in the networks and make the structure more spatially inhomogeneous.

E. Spectral dimension

While the geometric aspects of the fractal structures can be represented by the fractal dimension and mass correlation length, the spectral dimension d_s is a parameter commonly used to characterize the dynamic aspects of fractal objects, such as transport and relaxation properties. The number of vibration modes $N(\omega)$ of an object is related to the spectral density (density of states) $\rho(\omega)$ and vibration frequency ω by

$$N(\omega)=\int_0^\omega \rho(\omega')d\omega' \underset{\omega\to 0}{\propto} \omega^d, \tag{13}$$

where d is exactly the dimensionality of the object if it is Euclidean, but equals d_s for a fractal [19]. The spectral dimension of the DLCADEF network can be evaluated by the random walk analysis: a pointer is allowed to diffuse from one particle to a connected adjacent one at each step, starting

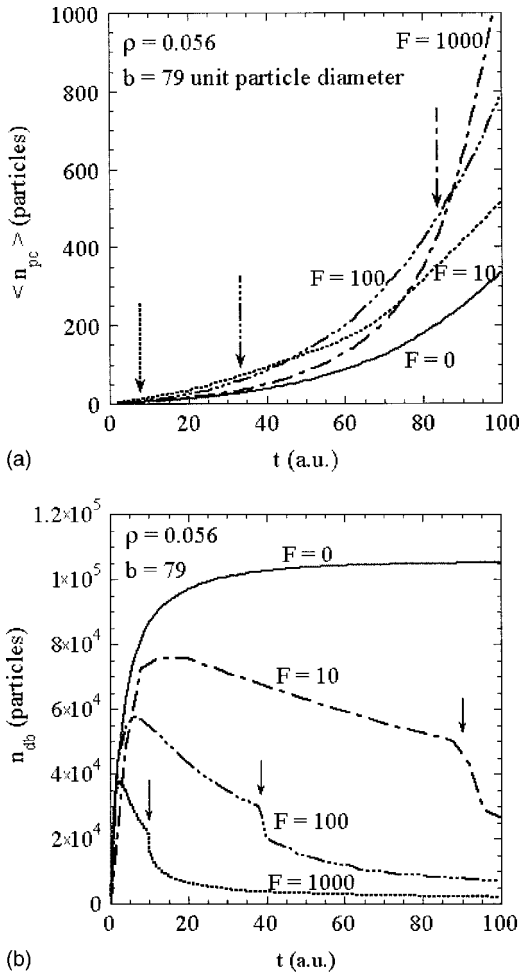

FIG. 3. (a) Evolution of average number of particles per cluster $\langle n_{pc}\rangle$ with time t (arrows denote t_{gel}). (b) Evolution of the number of dangling bonds n_{db} with time t (arrows denote t_{gel}, characterized by the sudden drop of n_{db}).

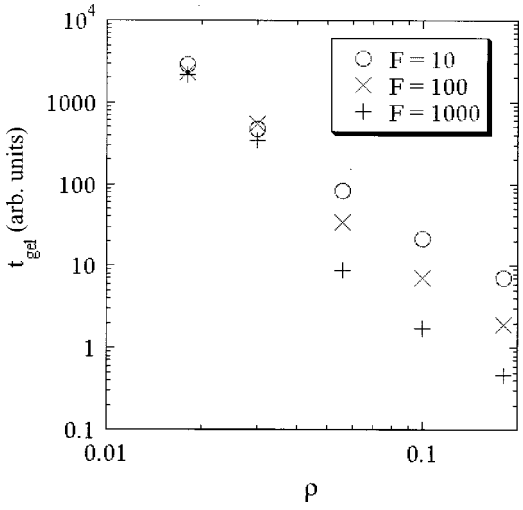

FIG. 4. Gel point t_{gel} vs density ρ for $F>0$ DLCADEF networks (the error bars are smaller than the size of the symbols).

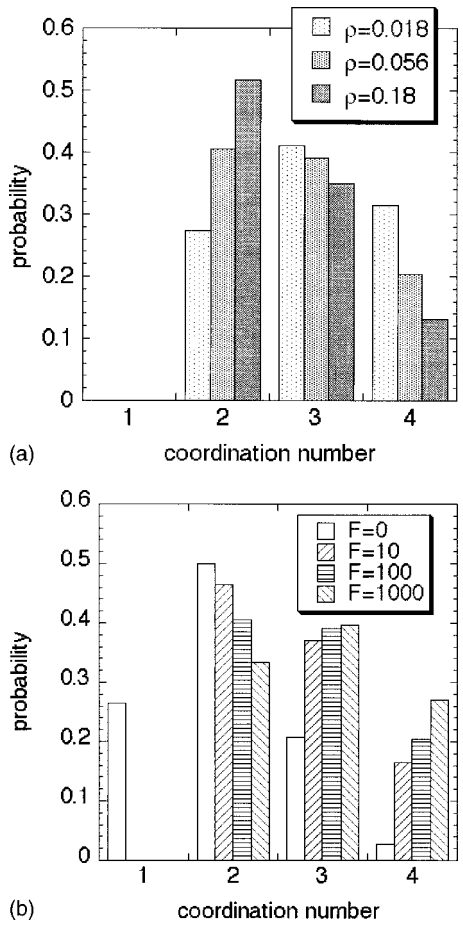

FIG. 5. (a) Probability distribution of the coordination number of the particles in the DLCADEF networks of $F=100$. (b) Probability distribution of the coordination number of the particles in the DLCADEF networks of $\rho=0.056$.

at any particle of the network. By the scaling argument [20], the mean square distance between the starting position and the current position $\langle R^2 \rangle$ is related to the number of steps n_s by

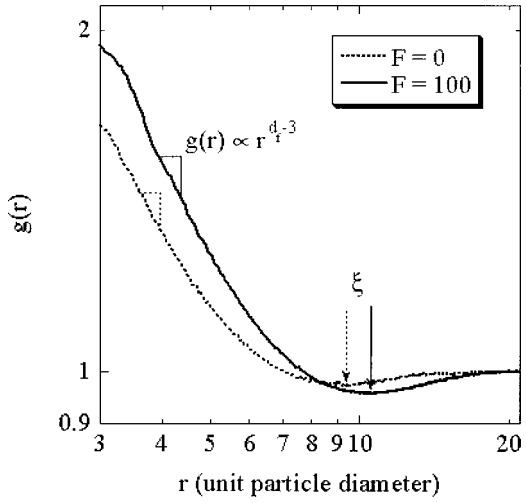

FIG. 6. Pair-correlation function $g(r)$ of DLCADEF networks at $\rho=0.03$ and $F=0,100$.

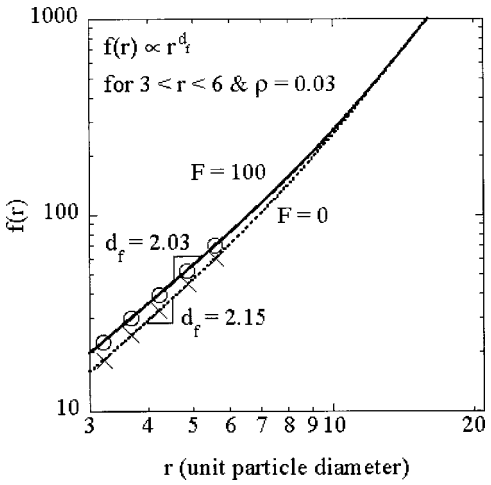

FIG. 7. Volume integral of pair-correlation function $f(r)$ of DLCADEF networks at $\rho=0.03$ and $F=0,100$.

$$\langle R^2 \rangle \propto n_s^{d_s/d_f}, \tag{14}$$

when $\langle R^2 \rangle$ is smaller than ξ^2, the upper size limit of the fractal regime.

The results of the random walk on two DLCADEF networks of $\rho=0.03$ is shown in Fig. 10, with one having $F=0$ and the other one having $F=100$. Each curve represents an average of all the particles as the starting point in one realization. For a Euclidean object, (d_s/d_f) equals 1. The mean square diffusion coverage $\langle R^2 \rangle$ for the DLCADEF networks increases much more slowly with the number of steps, as expected for their fractal nature. The exponent (d_s/d_f) is evaluated between $\langle R^2 \rangle = 9$ and 100 in this density level. The d_s of each individual DLCADEF network is calculated by multiplying the exponent (d_s/d_f) by the d_f obtained from $g(r)$. The dependence of d_s on ρ and F is illustrated in Fig. 11. The d_s is fairly independent of F, except at $\rho=0.018$

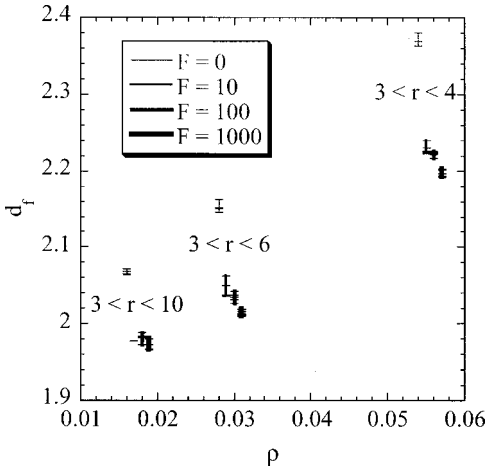

FIG. 8. Variation of fractal dimension d_f with density ρ for various P's of the DLCADEF networks. (For clarity, the data points are slightly spread along the ρ axis over their designated ρ, with smaller F towards the lower end and vice versa. The spread along the d_f axis refers to the spread of the model realizations. The range of r at each density represents the fractal regime where d_f is evaluated.)

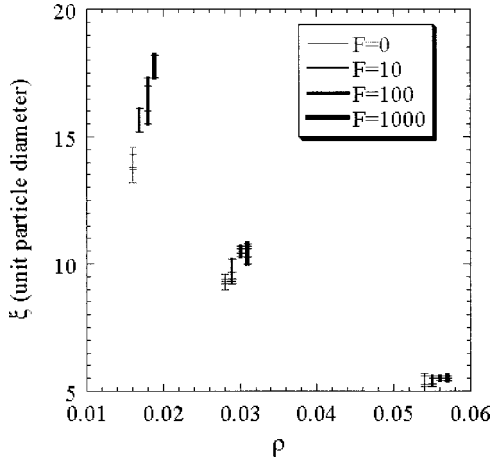

FIG. 9. Variation of correlation length ξ with density ρ for various F's of the DLCADEF networks. (For clarity, the data points are slightly spread along the ρ axis over their designated ρ with smaller F towards the lower end and vice versa. The spread along the ξ axis refers to the spread of the model realizations.)

where the d_s for $F=0$ is distinctly lower than those for the nonzero F's. By linearly extrapolating the d_s of $F=0$ towards $\rho=0$, which corresponds to the single-cluster limit of the DLCA model, $d_s \approx 1.1$ is recovered, which was demonstrated previously [21].

The validity of the derivation of d_s by the random walk algorithm is based on the fact that the spatial part of the diffusion equation is equivalent to that of the harmonic wave equation. However, because of that, the measured values are only the scalar approximation of the true d_s. Moreover, although the DEF model assumes deflections only occur at the dangling bonds, the origins of bond deflections and harmonic vibrations should be related. While the assumptions in the DEF model are effectively first-order approximations, the spectral dimension is nevertheless obtained as the characteristic exponent of the vibration spectrum of the whole resulting structure by treating every bond equally.

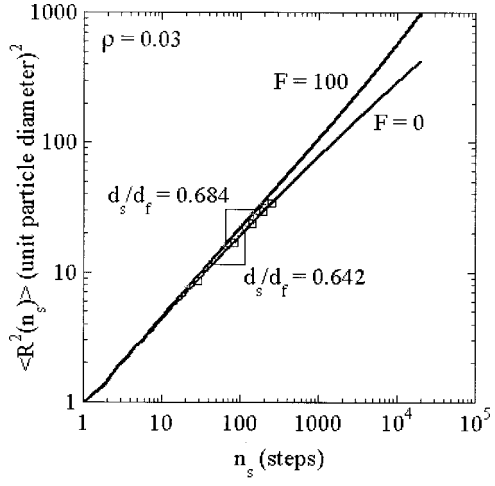

FIG. 10. Mean square diffusion distance $\langle R^2 \rangle$ against the number of steps n_s derived from the random walk analysis of two $\rho = 0.03$ DLCADEF networks at $F=0$ and 100, respectively.

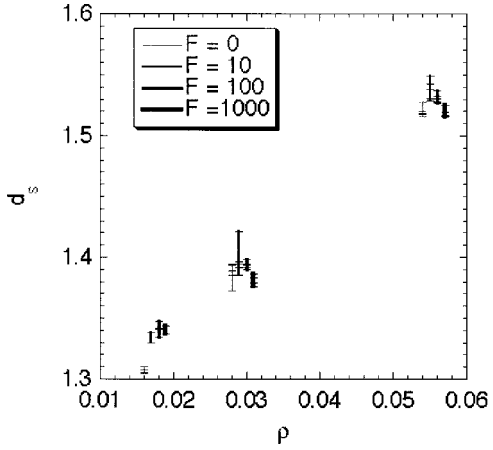

FIG. 11. Variation of spectral dimension d_s with density ρ for various F's of the DLCADEF networks. (For clarity, the data points are slightly spread along the ρ axis over their designated ρ with smaller F towards the lower end and vice versa. The spread along the d_s axis refers to the spread of the model realizations.)

IV. CONCLUSION

The DLCADEF model has shown close resemblance to the traditional DLCA in terms of the growth kinetics, fractal structure, and spectral dimension. Since the DLCA has been correlated to the real gels, such as aerogels in this context [1,16,18], the DLCADEF model should also be a suitable model of the gelation process. In addition, the dangling bond deflections create loops in the network. The extensive loop structure with negligible dead ends makes DLCADEF networks more physically realistic models for analysis of the structure and the mechanical properties of gels. The study of the mechanical properties of the DLCADEF networks has been published in Ref. [22].

The dangling bond deflection model, which principally simulates an intracluster reorganization, can be implemented with other types of kinetic aggregation models to simulate the sol-gel transition under different reaction conditions. However, there are no constraints imposed in the present model on the bond angles or the extent of deflection of dangling bonds. As a result, the degree of cyclic structure formation may be overestimated in the DLCADEF model. Such an effect is partially counteracted by the assumption in the DEF model that the bonds in the loops are considered as infinitely stiff regardless of the loop size. However, this assumption is in fact not physically realistic. More realistic aggregation model can be developed at the expense of computation time and with better understanding of colloidal phenomena.

ACKNOWLEDGMENT

The research was supported by U.S. Department of Energy research Contract No. DOE DEFG02-97ER45642. The core part of the algorithm was coded at the Université Montpellier II, and H.-S. Ma is grateful to R. Jullien and his group for their help during his month's stay there. The graphics of Fig. 2 were created by RasMac version 2.6, a free molecule

visualization program generously provided by Roger A. Sayle.

APPENDIX A: DERIVATION OF P_r

Consider two extreme and simplified cases: if the dangling branch is spherical and fractal (i.e., the density decreases from the center of the sphere towards the perimeter), and the vector pointing from the associated dangling bond to the center of the branch coincides with the axis of rotation, then the dangling bond deflection causes the dangling branch to rotate through an angle of θ rad. Assuming that the radius of the dangling branch is a, by the Debye expression [23] the rotational diffusion correlation time τ_r is

$$\tau_r = \frac{4\pi\eta a^3\theta}{3kT}, \tag{A1}$$

where η is the solvent viscosity and kT is the thermal energy. If the fractal dimension of the dangling branch is 2, the number of particles of unit diameter in the branch n_{pd} can be related to its radius a by

$$n_{\mathrm{pd}} = ha^2, \tag{A2}$$

where h is a proportionality constant of the order 1. Combining Eqs. (A1) and (A2) yields

$$\frac{1}{\tau_r} = \frac{3h^{3/2}kT}{4\pi\eta\theta}(n_{\mathrm{pd}})^{-3/2}, \tag{A3}$$

where the reciprocal of τ_r can be interpreted as the frequency of occurrence of the rotation as a function of n_{pd}.

If the bond-to-center vector is orthogonal to the axis of rotation, the dangling branch will circle around the axis. This trajectory involves moving the branch center along an arc of radius a and length λ, where

$$\lambda = a\theta. \tag{A4}$$

Since $\theta(=\pi/100) < \lambda$, especially when the dangling branch is large, the translational component of the trajectory is assumed to be the rate-limiting step. According to the Einstein-Smoluchowski equation [23], the translational diffusion coefficient D of a sphere is

$$D = \frac{\lambda^2}{2\tau_r^*}, \tag{A5}$$

where τ_r^* is the translational correlation time for rotation. The diffusion coefficient can be correlated to the sphere radius a by

$$D = \frac{kT}{6\pi\eta a}, \tag{A6}$$

which is called the Stokes-Einstein equation [23,24]. By eliminating D in Eqs. (A5) and (A6), and eliminating a and λ with Eqs. (A2) and (A4),

$$\frac{1}{\tau_r^*} = \frac{h^{3/2}kT}{3\pi\eta\theta^2}(n_{\mathrm{pd}})^{-3/2}, \tag{A7}$$

which has the same form as Eq. (A3) with different magnitude of the proportionality constant. Therefore, in both cases the frequency of occurrence ω_r scales with the number of particles in the dangling branch with an exponent of -1.5.

APPENDIX B: ESTIMATION OF F

For the translational Brownian diffusion, the translation correlation time τ_t can be evaluated by Eqs. (A5) and (A6), with λ set to 1 and τ_r^* substituted by τ_t (i.e., displacement by a unit particle diameter), and the final form is

$$\frac{1}{\tau_t} = \frac{\sqrt{h}kT}{3\pi\eta}(\eta_{\mathrm{pc}})^{-1/2}. \tag{B1}$$

The parameter F should be approximately the ratio of the coefficients in Eqs. (A3) and (B1), or Eqs. (A7) and (B1), which are

$$F \approx \frac{3h^{3/2}kT/4\pi\eta\theta}{\sqrt{h}kT/3\pi\eta} = \frac{9h}{4\theta} \approx O(10), \tag{B2a}$$

or

$$F \approx \frac{h^{3/2}kT/3\pi\eta\theta^2}{\sqrt{h}kT/3\pi\eta} = \frac{h}{\theta^2} \approx O(1000), \tag{B2b}$$

given that we chose $\theta = \pi/100$ in the simulation. Therefore the effect of F on the DLCADEF process was tested at $F = 10$, 100, and 1000.

[1] C. J. Brinker and G. W. Scherer, *Sol-Gel Science* (Academic, San Diego, 1990).

[2] G. C. Ruben, L. W. Hrubesh, and T. M. Tillotson, J. Non-Cryst. Solids **186**, 209 (1995).

[3] G. W. Scherer, D. M. Smith, and D. Stein, J. Non-Cryst. Solids **186**, 309 (1995).

[4] D. Stauffer, *Introduction to Percolation Theory* (Taylor & Francis, Philadelphia, 1985).

[5] T. Woignier, J. Phalippou, H. Hdach, G. Larnac, F. Pernot, and G. W. Scherer, J. Non-Cryst. Solids **147&148**, 672 (1992).

[6] P. Meakin, Phys. Rev. Lett. **51**, 1119 (1983).

[7] M. Kolb, R. Botet, and R. Jullien, Phys. Rev. Lett. **51**, 1123 (1983).

[8] R. Jullien and M. Kolb, J. Phys. A **17**, L639 (1984).

[9] W. Y. Shih, I. A. Aksay, and R. Kikuchi, Phys. Rev. A **36**, 5015 (1987).

[10] P. Meakin, J. Sol-Gel Sci. Technol. **15**, 97 (1999).

[11] R. Jullien and R. Botet, *Aggregation and Fractal Aggregates*

(World Scientific, Singapore, 1987).
[12] H.-S. Ma, J.-H. Prévost, R. Jullien, and G. W. Scherer, J. Non-Cryst. Solids **277**, 127 (2000).
[13] J. D. LeMay, in *Mechanical Properties of Porous and Cellular Materials*, edited by K. Sieradzki, D. J. Green, and L. J. Gibson, Mater. Res. Soc. Symp. Proc. No. 207 (Materials Research Society, Pittsburgh, 1991), p. 21.
[14] R. Jullien and A. Hasmy, Phys. Rev. Lett. **74**, 4003 (1995).
[15] A. Hasmy, É. Anglaret, R. Thouy, and R. Jullien, J. Phys. I **7**, 521 (1997).
[16] A. Hasmy, E. Anglaret, M. Foret, J. Pelous, and R. Jullien, Phys. Rev. B **50**, 6006 (1994).
[17] R. Vacher, T. Woignier, J. Pelous, and E. Courtens, Phys. Rev. B **37**, 6500 (1988).
[18] A. Hasmy, M. Foret, J. Pelous, and R. Jullien, Phys. Rev. B **48**, 9345 (1993).
[19] J.-F. Gouyet, *Physics and Fractal Structures* (Springer-Verlag, New York, 1996) Chap. 5.
[20] S. Alexander and R. Orbach, J. Phys. Lett. **43**, 625 (1982).
[21] R. Thouy, R. Jullien, and C. Benoit, J. Phys.: Condens. Matter **7**, 9703 (1995).
[22] H.-S. Ma, J.-H. Prévost, R. Jullien, and G. W. Scherer, J. Non-Cryst. Solids **285**, 216 (2001).
[23] P. W. Atkins, *Physical Chemistry*, 4th ed. (Oxford University Press, Oxford, London, 1990).
[24] R. B. Bird, W. E. Stewart, and E. N. Lightfoot, *Transport Phenomena* (Wiley, New York, 1960).